High Voltage Electron Microscopy Studies of Axoplasmic Transport in Neurons: A Possible Regulatory Role for Divalent Cations

MARK E. STEARNS
Department of Molecular, Cellular, and Developmental Biology, University of Colorado, Boulder, Colorado 80309

ABSTRACT Light and high voltage electron microscopy (HVEM) procedures have been employed to examine the processes regulating saltatory motion in neurons. Light microscope studies demonstrate that organelle transport occurs by rapid bidirectional saltations along linear pathways in cultured neuroblastoma cells. HVEM stereo images of axons reveal that microtubules (Mts) and organelles are suspended in a continuous latticework of fine microtrabecular filaments and that the Mts and lattice constitute a basic cytoskeletal structure mediating the motion of particles along axons. We propose that particle transport depends on dynamic properties of nonstatic microtrabecular lattice components.

Experiments were initiated to determine the effects of changes in divalent cation concentrations (Ca^{2+} and Mg^{2+}) on: (*a*) the continuation of transport and (*b*) the corresponding structural properties of the microtrabecular lattice. We discovered that transport continues or is stimulated to a limited extent in cells exposed to small amounts of exogenously supplied Ca^{2+} and Mg^{2+} ions (<0.1 mM). Exposure of neurons to increased dosages of Ca^{2+} and Mg^{2+} (0.2–1.0 mM) stimulates transport for 2–4 min at 37°C, but after a 5- to 20-min exposure the saltatory movements of organelles are observed gradually to become shorter in duration and rate until particle motion ceases to occur. HVEM observations demonstrated that Ca^{2+}- and Mg^{2+}-stimulated changes in the organization of the microtrabecular lattice are associated with the cessation of motion. Ca^{2+}-containing solutions produced contractions of the microtrabecular filaments, whereas Mg^{2+}-containing solutions had the opposing effect of stimulating an elongation and assembly (expansion) of microtrabeculae. On the basis of these observations we hypothesize that cycles of Ca^{2+}/Mg^{2+}-coupled contractions and expansions of the microtrabecular lattice probably regulate organelle motion in nerve cells.

Although it is widely acknowledged that intracellular transport depends on the architectural properties of nonmuscle cell systems, the basic regulatory mechanisms remain enigmatic. The rapid transport of organelles in neurons represents one of the more spectacular examples of cytoplasmic granule movement that has been investigated. In this system, light microscope observations have revealed that organelles in neurons move bidirectionally in a rapid, saltatory manner along linear pathways in the axon (13, 14, 31, 37, 44, 55). Electron microscopy evidence (1, 15, 26, 47, 50) and drug studies (1, 12, 27, 33) have indicated that either axoplasmic microtubules (Mts) or microfilaments (Mfs) probably mediate this particle transport.

It is uncertain, however, whether these filamentous elements, functioning alone or in cooperation, are sufficient to produce the orderly motion of cellular components. Byers (7), for example, has reported that exposure of axons to colchicine, at levels that drastically reduce the numbers of Mts, does not appear to interfere with the continued transport of radioactively labeled material. She interpreted the data to mean that a component other than Mts may be directly involved in the regulation of fast axonal transport. Recent experiments with neurons incubated in high Ca^{2+} solutions (3) have provided added support for her suggestion that Mts are not required for fast transport. The conclusion contradicts several reports in which the use of antimicrotubule drugs has provided convincing evidence that intact Mts are required for fast transport (12,

THE JOURNAL OF CELL BIOLOGY · VOLUME 92 MARCH 1982 765-776

26, 47). In fact, several models that directly implicate Mts in the regulation of transport have been proposed (6, 42, 43, 46, 47). The opposite nature of the conclusions reached would indicate that further work is required to resolve the roles of filamentous structures in fast transport.

The main difficulty with the above studies is that the antimitotic drugs (colchicine, podophyllotoxin, vinblastine, and Ca^{2+}) tend to affect numerous physiological processes unrelated to Mts (10, 16, 17, 52, 53, 56). In addition, attempts to relate mechanisms of transport to the properties of specific structures have been complicated by the fact that neurons contain varying amounts of diverse fibrous components, including Mts, Mfs, neurofilaments (Nfs), myosin, and sulfated mucopolysaccharides from which nerve cells might construct alternative transport systems. Burton and others (6, 27, 35, 40, 51), for example, have found that Mts and Nfs are coated with a fine meshwork of anastomosing filaments. Since the filaments can be stained with alkaline dyes (ruthenium red, lanthanum, and alcian blue) reactive for mucopolysaccharides, the authors have suggested that Ca^{2+}-sensitive contractile properties of these components might regulate fast axonal transport in nerve cells, an intriguing concept that deserves further attention.

High voltage electron microscopy (HVEM) stereo techniques have been developed recently by Porter and colleagues (4, 5, 54) for examining the three-dimensional organization of the cytoplasmic matrix. From thick section studies of nerve tissue they have reported that Mts and organelles are embedded in a latticework of space-filling, anastomosing filaments, termed microtrabeculae (11). HVEM studies of whole-mount pigment cells have further revealed that cycles of pigment granule aggregation and dispersion rely on morphological transformations (contractions and energy-dependent expansions) of the microtrabecular components in which Mts and granules are suspended (8, 39). On the basis of these types of studies, Ellisman and Porter (11) have recently proposed that similar, albeit less dramatic, changes in lattice organization may function to regulate vesicle motion in neurons.

In this paper we have investigated the ultrastructural properties of components associated with organelle transport in cultured neuroblastoma (C1300) cells, used as a model nerve cell system. The studies have been extended to investigate the possible role that divalent cations (Ca^{2+} and Mg^{2+}) might play in axonal transport. We have examined the correlative effects that exogenously supplied ions can have on both the continuation of transport and the corresponding organizational properties of cytoskeletal components mediating movement. With these results we have constructed a model describing the role of the microtrabecular lattice in fast axonal transport.

MATERIALS AND METHODS

Culture Procedure

The rat neuroblastoma (C1300) cell line was a gift of Dr. N. W. Seeds, University of Colorado Medical School, Denver, Colorado. Cells were grown to log phase in Dulbecco's modified eagle's medium (DMEM) containing 10% fetal calf serum (FCS) and plated on Formvar-, carbon-coated gold grids (400-mesh) supported on glass cover slips or plated directly on glass cover slips. Neurons were induced to form axonal extensions over 4–6 d in DMEM containing 1% FCS according to methods of Seeds et al. (48). The cultures were maintained at 37°C in an atmosphere of 5% CO_2 and 95% air.

Experimental Procedure

Before treatment with experimental agents, the cell medium was gently replaced by several changes of modified Hanks' balanced salt solution (mHBSS), made free of divalent cations and containing 0.1-mM levels of EGTA and EDTA, pH 7.3.

Cells on the cover slips were then transferred to a slide for examination with a Zeiss Universal microscope. Cover slips were mounted in mHBSS, and cells were separated from the slide with cover slip spacers. Valap (1:1:1, Vaseline: lanolin:paraffin) was used to seal two sides of the cover slip and reduce evaporation of the medium. The slides were kept warm with an air curtain stage incubator set at 37°C. Solutions at 37°C were exchanged by sequentially adding about five drops on one side of the cover slip while absorbing solution with Kimwipes on the other side. The response of cells was recorded by phase-contrast cinematography at 120 frames/min, and films were analyzed with a stop-motion projector. The average rates of particle motion were determined from measurements of the distances moved with time of 200 organelles in stop-motion studies of films.

Solutions

In experimental treatments, cells were washed with several changes of mHBSS and exposed by three volume changes in freshly made mHBSS containing known amounts of added Ca^{2+} and Mg^{2+} ion and ionophore. Both 1 μg/ml A23187 and 13 mM NaH_2PO_4 (2) function effectively as divalent cation ionophores, and the effects of ions on transport were tested in the presence of both agents. The ability of exogenously added Mg^{2+} ions to affect cell structure was tested further using the magnesium ionophore, dicyclohexylcarbodiimide (DCCD), in mHBSS containing increased levels of Mg^{2+} ion (18). Control studies were carried out utilizing Ba^{2+}, Sr^{2+}, Co^{3+}, Mn^{2+}, Ni^{2+}, and Cu^{2+} ions in place of Ca^{2+} and Mg^{2+}.

In some studies, the neurons were washed and exposed to 1-mM levels of EDTA or EGTA (Sigma Chemical Co., St. Louis, MO) in mHBSS containing ionophore. After exposure to EGTA and EDTA for 20 min, neurons were transferred to mHBSS containing 13 mM NaH_2PO_4 and increasing amounts of Ca^{2+} and Mg^{2+} by five changes of the solution volumes. Recovery of transport was qualitatively determined from light microscope studies of at least 10 different cells.

A23187 was obtained from Dr. R. Hamill, Eli Lilly Co., Indianapolis, IN, and was dissolved in dimethyl sulfoxide (DMSO) to give a stock solution of 1 mg/ml. The ionophore was added to the test solutions just before the experiments. The final concentration of DMSO did not exceed 0.1%. In control experiments with solutions of 0.1% DMSO, cell behavior and ultrastructural properties were not affected. The pH was routinely adjusted to 7.3 with dilute NaOH or HCl and the osmolarity adjusted to ~325 mosM with NaCl.

HVEM Procedures

During examination in the light microscope, neurons grown on gold grids were fixed with drops of 2.9% glutaraldehyde in mHBSS at 37°C for 30 min. Cells were then washed three times with HBSS, postfixed with 1% osmium tetroxide for 3 min at 4°C, and washed with HBSS. After three rinses in distilled water, cells were dehydrated in a graded acetone series and dried by the critical-point method. Cells were lightly coated with a layer of carbon and stored in a vacuum dessicator for up to 2 wk. The neurons were examined under an accelerating voltage of 1,000 kV. The whole-cell fixation procedure used is similar to that described by Wolosewick and Porter (54).

The sizes of the microtrabeculae were determined from samples experimentally treated for 20 min and fixed for HVEM. The data (Table I) represents

TABLE I

Measurements of Microtrabecular Lattice Associated with Mts

Treatment	Diameters	Lengths
	nm	*nm*
mHBSS	5.1 ± 2.2	180 ± 22
0.10 mM Ca^{2+}	7.5 ± 3.1	163 ± 16
1.0 mM Ca^{2+}	17.1 ± 6.3	93 ± 21
0.10 mM Mg^{2+}	6.1 ± 1.1	195 ± 31
2.0 mM Mg^{2+}	3.3 ± 0.9	272 ± 65

Summary of measurements of the sizes of microtrabeculae in axons of neurites exposed to exogenously supplied Ca^{2+} and Mg^{2+} ions for 20 min (at 37°C) in mHBSS containing 1 μg/ml A23187. In comparison to trabeculae in control cells, the trabeculae in Ca^{2+}-treated (1 mM) neurons are observed to dramatically increase in average diameter by about fourfold and decrease in their length by one half. In contrast, the trabeculae decreased in diameter by about one half and increased in length by about one third in the Mg^{2+}-treated (2 mM) neurites. The results for each data point given represent values averaged ± SE from measurements of 100 or more trabeculae in three different cells from separate experiments.

measurements that were averaged from 100 or more trabeculae examined in three separate samples for each experiment. For these calculations, thin areas of the axon near the base of the growth cone were photographed in stereo at × 25,000. The negatives were printed at × 100,000, and the diameters and lengths of trabeculae found coating the surfaces of the microtubules were measured in a stereo viewer with a vernier caliper.

RESULTS

Light Microscope and HVEM Correlative Studies

The motion of organelles (lipid, lysosomal, and smooth endoplasmic reticulum [SER] vesicles) in neurons was followed with time-lapse phase microscopy. Stop-motion analysis of movement of 200 particles showed that they move by rapid saltations (0.5–9 μm/s) in a bidirectional fashion along axons. Further slow-motion studies of these films indicated that the motion of individual particles is subject to localized control, in that transport usually occurs along relatively linear axoplasmic tracts (Figs. 1 and 2). For example, nearby particles are often observed to move simultaneously in opposing directions along adjacent axoplasmic tracks (Fig. 2). In general, though, a given particle's motion is continuous in one direction for a series of saltation events extending along the length of the axon (Figs. 1 and 2). Many of these organelles accumulate in the growth cone and lamellar regions, where they are seen to continue streaming, albeit in a nonlinear, stochastic fashion. Interestingly, in developing regions of the growth cone, clusters of these particles are sometimes observed suddenly to stop moving and then move *en masse* to fill newly spread lamellar structures of the growth cone. Light studies of 350 lamellae demonstrated that most (311 or 89%) lamellae are normally active in particle transport, although some lamellae (39) were not involved in organelle motion.

HVEM pictures of fixed and critical-point-dried neurons reveal that the axoplasmic matrix consists primarily of aligned microtubules and a continuous space-filling microtrabecular lattice (MTL) in which the Mts and organelles are suspended (Figs. 3–5). Figs. 3–5 show that a fine network of the microtrabecular filaments (5.1 nm diameter) fill spaces between the Mts and organelles and serves to interconnect Mts with other Mts and Mts with the suspended organelles in both axonal (Fig. 4) and growth cone regions (Fig. 5) of the cell. When lamellae, or spreading regions of cells, were examined at the ultrastructural level, 280 of 311 (90%) of those known to be involved in organelle transport at the time of fixation contained Mts in close association with the organelles. The 39 lamellae not involved in transport contained a fine meshwork of trabecular filaments, of which only five lamellae (or 13%) contained any recognizable Mts, indicating that microtubules and their associated lattice components are important for organelle transport.

In this regard, we observed that some neurites contain centralized cores of Mts and that the remaining axoplasmic area is filled with the MTL. Light microscope and HVEM studies of these cells demonstrated that the transport of organelles is localized in the regions defined by the Mt bundles and that transport does not occur in regions containing strictly the MTL component.

Divalent Cation Effects

Neurons washed in mHBSS containing the ionophoric agents A23187 (1 μg/ml) or 13 mM NaH_2PO_4 (2) plus low levels of added Ca^{2+} and Mg^{2+} ions (0.05–0.1 mM) did not exhibit significant changes in their cell shape or transport activities over the pH range of 6.8–7.5 tested. If the amount of A23187 used is increased to 5 and 10 μg/ml concentrations, the cells react by rapidly retracting their extended axons, and HVEM studies show that A23187 at 10 μg/ml levels produces a contracted lattice. Thus, in all the experiments reported here, 1 μg/ml A23187 or 13 mM NaH_2PO_4 was employed in order to minimize the independent effects of these agents, since under these conditions little or no detachment and/or retraction of the neurites occurred. In all the studies reported, identical results were obtained in experiments using either of these ionophoric agents.

Time-lapse studies of the treated cells show that particle motion is stimulated in rate and amount in neurons exposed to Hanks' solutions containing small amounts of either Ca^{2+} or Mg^{2+} cations (<0.1 mM) over a pH range of 6.8–7.5. At increased levels of either Ca^{2+} (0.2–1.0 mM) or Mg^{2+} ions (0.5–2.0 mM) tested, the ions exert a dose-dependent effect on both cell shape (Fig. 6) and the rates of axonal transport (Table II). We found that the initial influx of these ions into cells stimulates transport, but that, with time, the motion of particles becomes noticeably irregular and jerky, and in many cases motion finally ceases altogether. At even higher Ca^{2+} levels (2–20 mM), transport invariably came to a rapid halt by 2–5 min. In addition to the effects on transport, Ca^{2+} induces a retraction of lamellae extensions apparently as a result of contractions of the axoplasmic matrix (compare Fig. 1*a–c*, *h*, and *i* with Fig. 1 *d–f*).

In comparison to the Ca^{2+} ion effects, high Mg^{2+} levels (5–20 mM) stimulate the formation of lamellae, and cells often exhibit some irregular, sporadic transport activities after 20 min at 37°C. Note that, in very large axons containing numerous mitochondria, some transport still continues in the presence of added Ca^{2+} or Mg^{2+}, even at the 20-mM levels tested.

Control Studies

In control studies, we found that the substitution of other metal ions (Ba^{2+}, Mn^{2+}, Co^{3+}, Sr^{2+}, Ni^{2+}) at 0.5- and 1.0-mM levels for Ca^{2+} and Mg^{2+} ions does not have an effect on the continuation of transport. Excess Co^{3+} and Sr^{2+} at 10-mM levels has an inhibitory effect on transport. For some experiments, neurons were preincubated in mHBSS containing either Mg^{2+} or Ca^{2+} ions at 0.1-mM levels for 1 min, and the cells were immediately transferred to mHBSS solutions containing the opposing divalent ion (Ca^{2+} or Mg^{2+}) at 1- and 2-mM levels (Table II). In these studies, we observed that the time interval required for transport to slow down or halt in response to added Ca^{2+} and Mg^{2+} was approximately doubled from the time periods recorded for experiments in Table II, where the preincubation step was omitted.

Finally, to further convince ourselves that an influx of Ca^{2+} into the cells was in fact responsible for the results recorded in Table II, neurons were exposed to 10 mM Ca^{2+} for 5 min in Hanks', and these cells were transferred to mHBSS containing A23187. Transport activities in the neurons came to a halt after relatively short incubation periods of 3–5 min in the A23187 solutions, indicating that membrane-bound Ca^{2+} was entering the cells. Alternatively, when the cells were preexposed to La^{3+} ions (1.0 mM) for 5 min, the transport of particles continued unabated when the neurons were subsequently transferred to ionophore solutions containing 1.0 mM Ca^{2+}. The experiments indicate that La^{3+} ions bind to membrane binding sites specific for Ca^{2+} transport, preventing A23187-mediated Ca^{2+} uptake.

For some studies with Mg^{2+} ion, the Mg^{2+} ionophore DCCD (10 μm) was substituted for A23187. Results identical to those reported in Table II using A23187 are obtained from experiments with DCCD.

HVEM Studies of the Divalent Cation Effects

When the neurons were exposed to either low Ca^{2+} and Mg^{2+} levels (0.1 mM) or briefly exposed (1 min) to high doses (1-mM levels) of Ca^{2+} and Mg^{2+}, the ultrastructural organization of the axoplasm generally remained unchanged from that seen in the untreated cells (Figs. 3–5). However, in neurons exposed to increased Ca^{2+} ion concentrations (0.2–1.0 mM) for

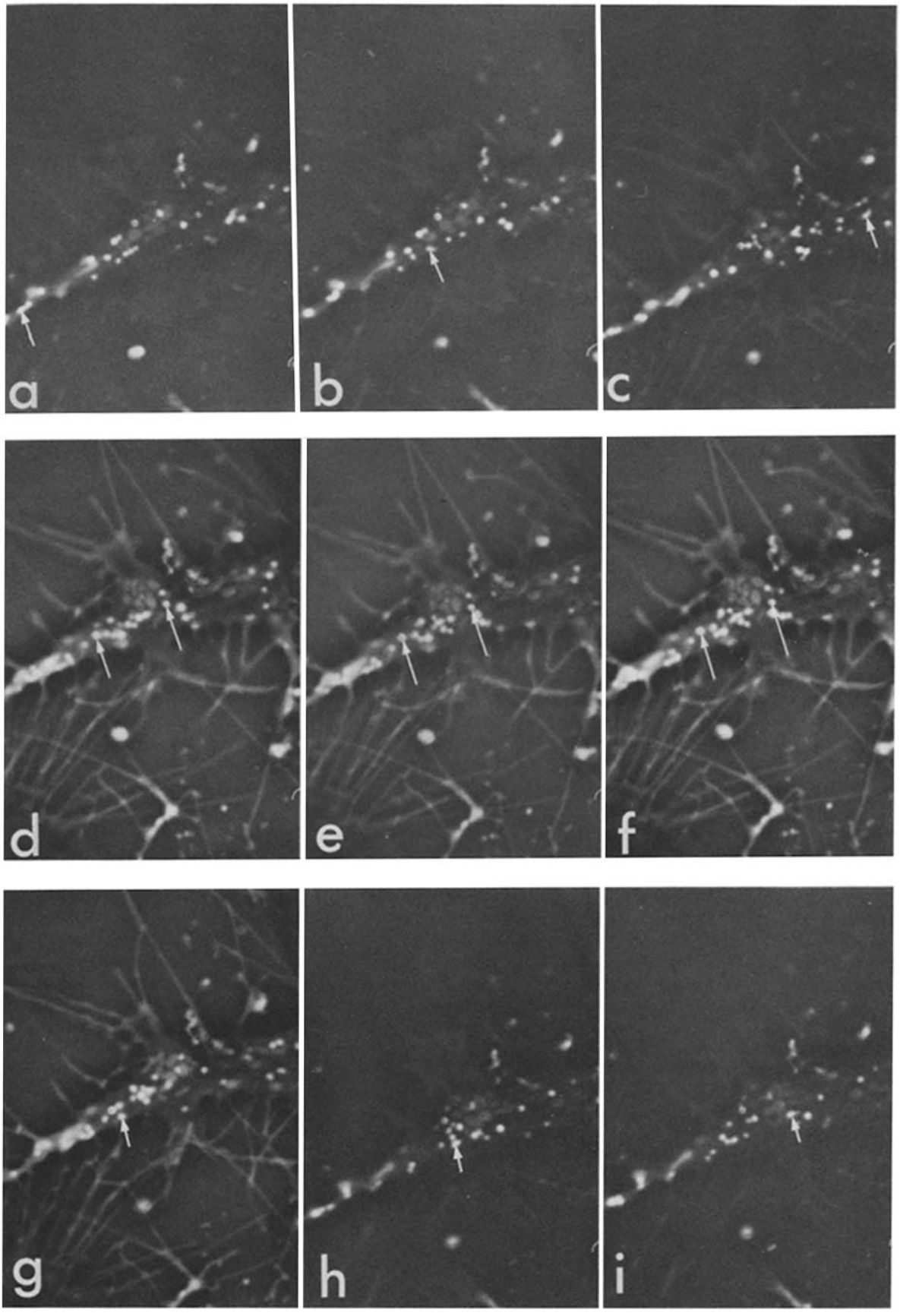

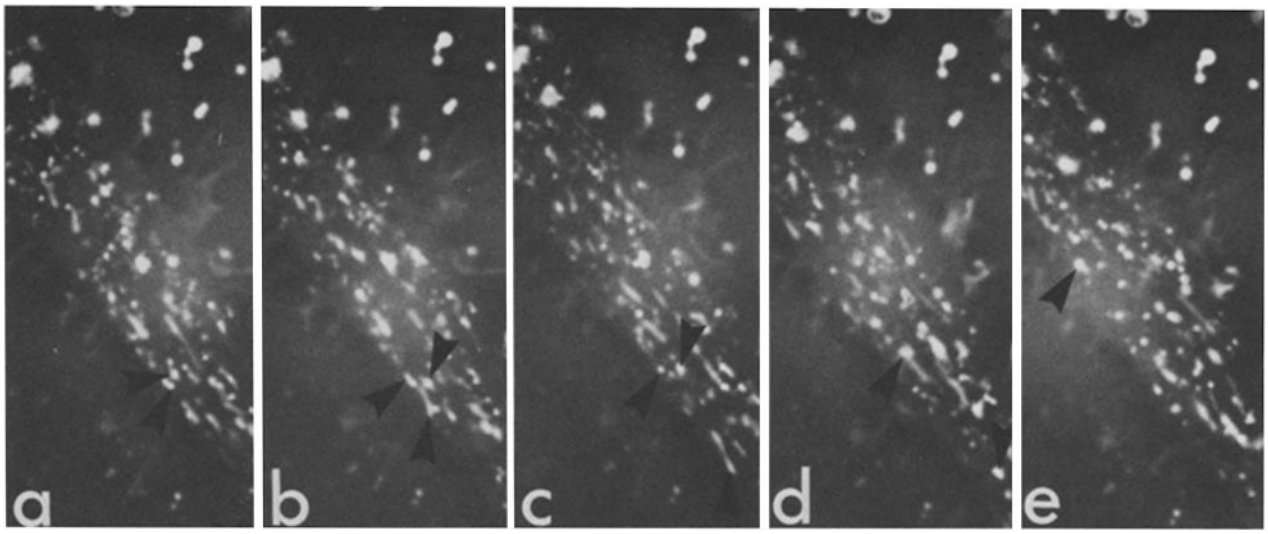

FIGURE 2 Phase time-lapse sequences showing two closely associated particles (*a–c*) which were observed to simultaneously move in opposite directions (*d* and *e*) along linear pathways in the axon. × 2,700.

relatively long time periods, HVEM studies (Figs. 6–8) show that coincident with retractions of lamellae (Fig. 1) the microtrabecular lattice gradually becomes more coarsely divided. The individual microtrabeculae associated with the Mts (Fig. 8) and organelles (Figs. 7 and 8) become thickened in appearance (17.1 nm) as compared with the diameters of trabeculae in controls (compare Figs. 4 and 5 with Figs. 7 and 8; see Table I). In addition, the intertrabecular spaces simultaneously increased in size to about double their control values. Associated with these changes in trabecular conformation and lattice organization, the axonal microtubules in Ca^{2+}-treated cells were often found to align in closely appressed parallel arrays (Fig. 8).

Exogenously added Mg^{2+} ions (0.5–2 mM) caused neurons gradually to spread and form new lamellipodia. In contrast to the Ca^{2+} ion effects, the lattice in these cells was more finely divided and exhibited increased numbers of thin, elongate trabeculae (Table I). The surfaces of both the Mts and particles were coated with numerous thin filaments (Fig. 9). Compare Fig. 9 with Figs. 4 and 5 of controls and Figs. 7 and 8 of Ca^{2+}-treated cells. In the newly forming lamellar regions, the trabeculae and bundles of Mts and Mfs appeared in the process of assembly and elongation. The addition of nonspecific metal ions (Ba^{2+}, Sr^{2+}, Co^{3+}, Mn^{2+}, Ni^{2+}, Cu^{2+}) at 1-mM levels in place of Ca^{2+} and Mg^{2+} did not have similar effects, indicating that a specific fluctuation of Ca^{2+} and Mg^{2+} ions plays an important role for transport-related activities of the lattice. The above Ca^{2+}/Mg^{2+} experiments were carried out simultaneously on three specimens for each experiment, and the samples were prepared for HVEM under identical conditions to eliminate possible interpretational errors that may arise from the preparative steps.

Divalent Chelator Experiments

In attempts to further determine what importance divalent cations might play in the regulation of transport, neurons were exposed to 1-mM amounts of the cation-chelating agents EDTA and EGTA in the presence of A23187 (see Materials and Methods). From time-lapse studies we found that cells exhibit both an increased amount of ruffling and transport activity during the first 5 min of treatment. After 20 min of continuous exposure, however, the spreading lamellae are essentially frozen in an extended form and organelle transport is either discontinued or at least limited in its extent. In stereo HVEM images, the lattice in the EDTA- or EGTA-treated cells appears coarsened and distorted in appearance, somewhat resembling that in the Ca^{2+}-treated cells (Figs. 7 and 8). These changes in lattice organization are especially apparent after the exposure of cells to EGTA solutions for 20 min. Thus, the removal of either free Ca^{2+} or Mg^{2+} ions from the axoplasm seems to disturb ion balances necessary for the maintenance of a structurally and functionally sound lattice. When increased amounts of EGTA and EDTA (3 and 10 mM, respectively) are employed in the experiments, the axonal extensions detach from the substrate and rapidly retract into the cell body.

Table III shows time intervals required for the recovery of transportation neurons after the inhibition of transport with 1 mM EGTA and EDTA solutions. In general, we found that transport recovery times are reduced to a minimum, as judged by observations made on at least 10 different cells in each

FIGURE 1 Phase time-lapse sequence taken at 2-s intervals of particle transport along an axon. Frames *a–c* show normal transport in a neuron in mHBSS; one of the particles (arrows) is marked to demonstrate its unidirectional motion along a linear pathway over a 4-s interval. Frames *d–f* show that transport is discontinued after 5-min exposure of the axon to mHBSS containing 13 mM NaH_2PO_4 and 1 mM Ca^{2+} ions. Arrows mark particles in frames *d–f* to show that no motion has occurred. Frames *g–i* show the same axon during recovery from Ca^{2+} inhibition of transport in mHBSS free of Ca^{2+} ions. Arrows in frames *g–i* mark a particle that is beginning to move along the axon. Concomitant with the Ca^{2+} ions, a reversible arborization of the axonal lamellipodia occurs. This occurs as a result of the Ca^{2+}-triggered contractions of the microtrabecular lattice which simultaneously prevent the continuation of organelle motion. During recovery of the onset of particle motion the lattice reexpands, permitting the onset of transport and lamellae spreading. × 3,000.

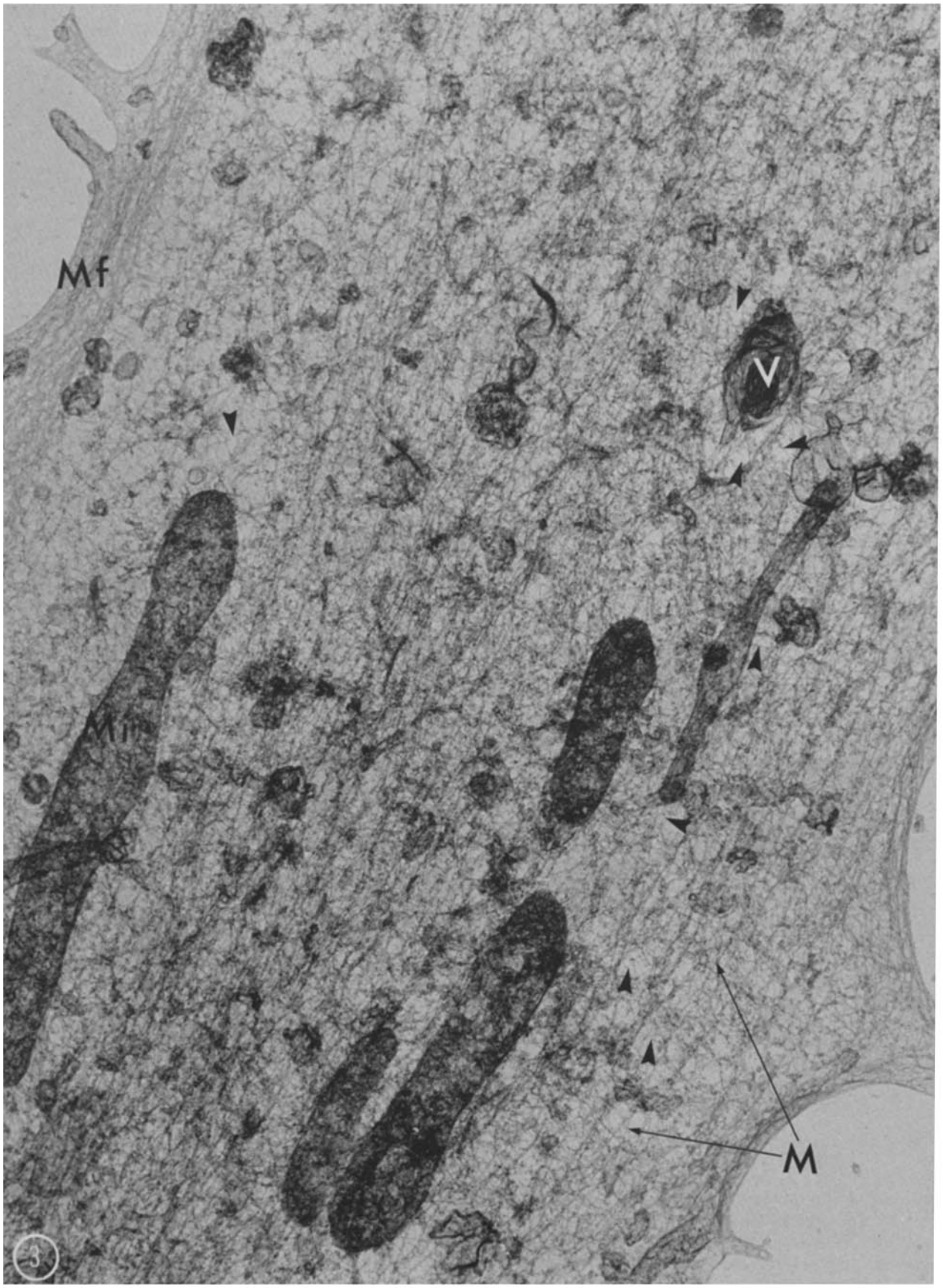

FIGURE 3 View of part of an axon showing microfilament bundles (*Mf*) near the subplasmalemmal surface and numerous microtubules (*M*) throughout the axoplasmic matrix. *V*, vesicle. Microtubules and organelles are suspended in a fine cross-linking network of filamentous material, the microtrabecular lattice (arrowheads). An area from Fig. 3 is shown at a higher magnification in stereo in Fig. 4. × 35,000.

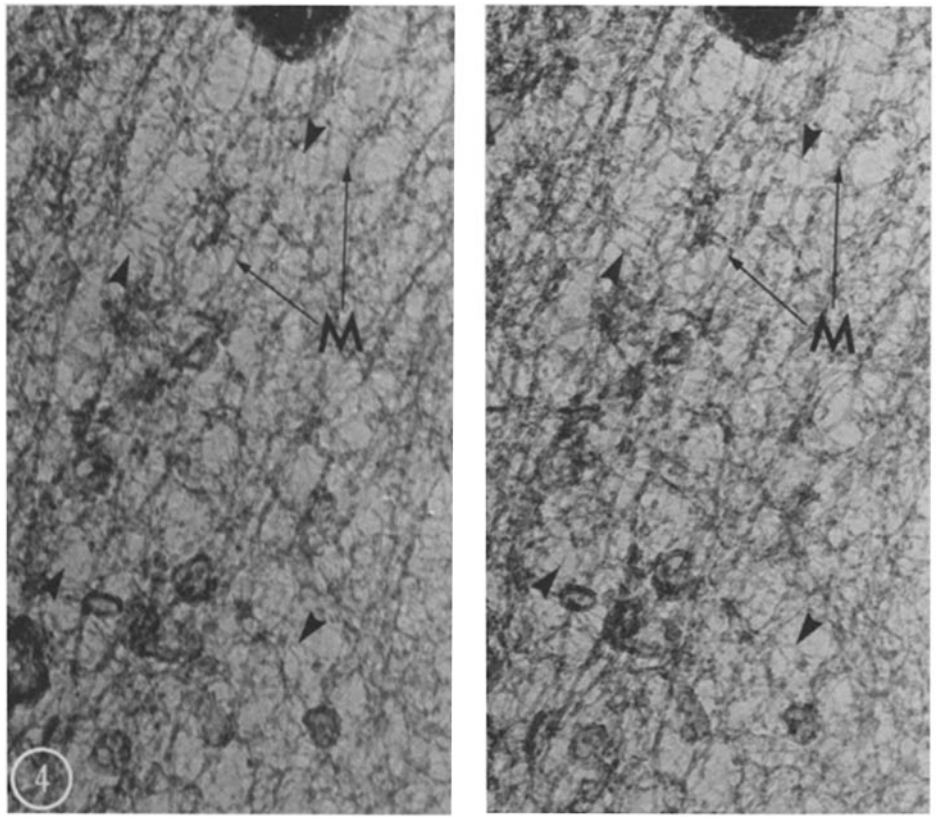

FIGURE 4 Stereo pair showing a three-dimensional array of aligned microtubules (*M*) suspended in a cross-linking lattice work of trabeculae (arrowheads). *V*, vesicle. In these thick regions of the axon, a superimposition of structural information makes it difficult to determine organizational patterns of the microtrabeculae networks. For proper viewing of stereos, a stereo viewer should be employed. × 114,000.

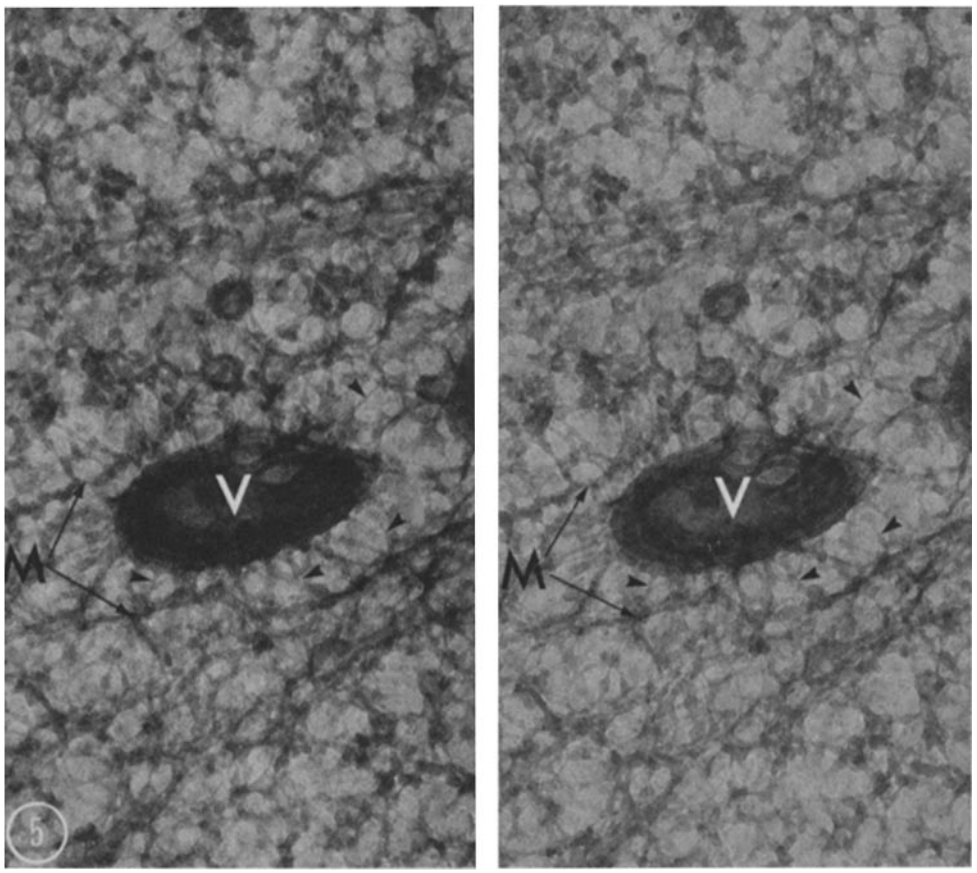

FIGURE 5 Stereo pair showing part of a growth cone region of a neurite. A vesicle (*V*) is seen in close juxtaposition with microtubules (*M*). The microtrabeculae (arrowheads) form a prominent continuous latticework in this region of the cell and appear to cross-link the surfaces of the particle with the microtubules. × 90,000.

preparation, if low levels of Ca^{2+} and Mg^{2+} (0.05 mM) are added to a recovery buffer of mHBSS with 13 mM NaH_2PO_4. When higher Ca^{2+} and Mg^{2+} (0.2 mM) levels are used in the buffer, recovery times are reduced to 2 min, but transport is subsequently observed to halt by ~5–10 min. HVEM studies reveal that the lattice in these neurons is contracted in Ca^{2+}

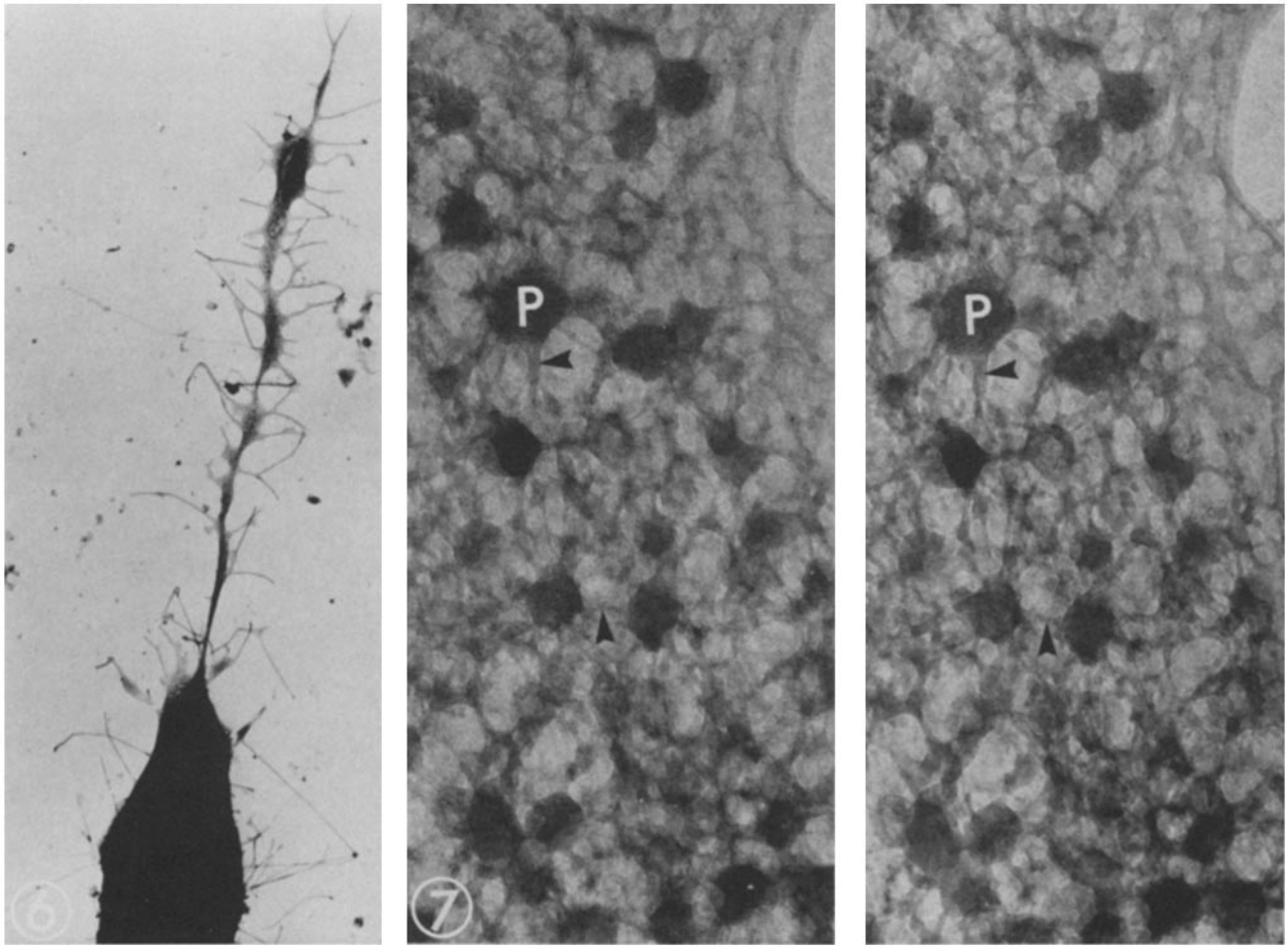

FIGURE 6 High-voltage image of whole cell after exposure to 1 mM Ca^{2+} for 5 min. The cell axon is arborized as a result of the retraction of growth cone and lamellae extensions. Transport was stopped at the time of fixation. × 2,000.

FIGURE 7 Stereo view of a region of the growth cone in Fig. 6. The lattice is coarsely divided by thickened trabecular fibers (arrowheads) that are often seen attached to the surfaces of particles (*P*). Intertrabecular spaces are generally larger. This "contraction" state of the lattice trabeculae appears to interfere with the continuation of transport. × 75,000.

TABLE II

Effects of Divalent Cations on Particle Transport in Neurons

Treatment	Effect	Recovery
mM	*min*	
HBSS ± Ca (no ionophore)	+	
0.05 Ca + 0.10 Mg	+ (Optimal)	
0.05–0.10 Ca	+	
0.20–0.40 Ca	−, 20	+20
0.60–1.00 Ca	−, 5–10	+20
2.00–20.00 Ca	−, 2–5	−30
0.05–0.10 Mg	+	
0.50–2.00 Mg	−, 10–20	+10
5.00–20.00 Mg	+/−, 20	+10
0.10 Mg → 1.00 Ca	−, 15	+20
0.10 Ca → 2.00 Mg	−, 30	+10

Summarizes the effects of exogenously supplied Ca^{2+} and Mg^{2+} ions on the continuation of organelle transport. (+) denotes no effect; (−) means that transport was stopped in the time interval indicated. The data represent the average results obtained from 10 different experiments using mHBSS containing 13 mM NaH_2PO_4 and 1 μg/ml A23187. Recovery from the experimental treatment was in mHBSS made free of divalent cations. (+) denotes recovery in the time indicated. In some experiments (bottom column), cells were exposed to low Mg^{2+} or Ca^{2+} for 1 min, then transferred to a solution containing the opposing ion in order to measure the subsequent effects which exogenously supplied Mg^{2+} and Ca^{2+} ions could exert on transport.

buffers and expanded or gelated in Mg^{2+} buffers. In control experiments, the substitution of $Ba^{2+}/Mn^{2+}/Co^{3+}/Sr^{2+}$ (0.2 mM) for Ca^{2+} and Mg^{2+} ion does not decrease the recovery times required. In fact, the exposure of cells to high levels of Co^{3+}/Sr^{2+} (10 mM) or La^{3+} (1 mM) ions inhibits the recovery of transport, again indicating that Ca^{2+} ions are required for axonal transport since these ions are known to block the entry of exogenously supplied Ca^{2+} ions.

DISCUSSION

Intracellular motility in neurons depends on properties of an asymmetrically structured cytoskeleton. The results presented in this paper demonstrate that developing axons of neuroblastoma cells consist of parallel arrays of Mts and organelles suspended in a cross-linking lattice of microtrabeculae. Ellisman and Porter (11) have recently reported similar results from HVEM thick section studies of mature rat nerves where they observed that cross-bridging filaments coat the surfaces of Mts, NFs, and vesicles. The data indicate that microtrabeculae in association with Mts or Nfs form a functional cytoskeletal structure for controlling the transport of organelles along axons. We believe that subtle changes in the organization of nonstatic lattice components must mediate saltatory movements along pathways defined by Mts or Nfs.

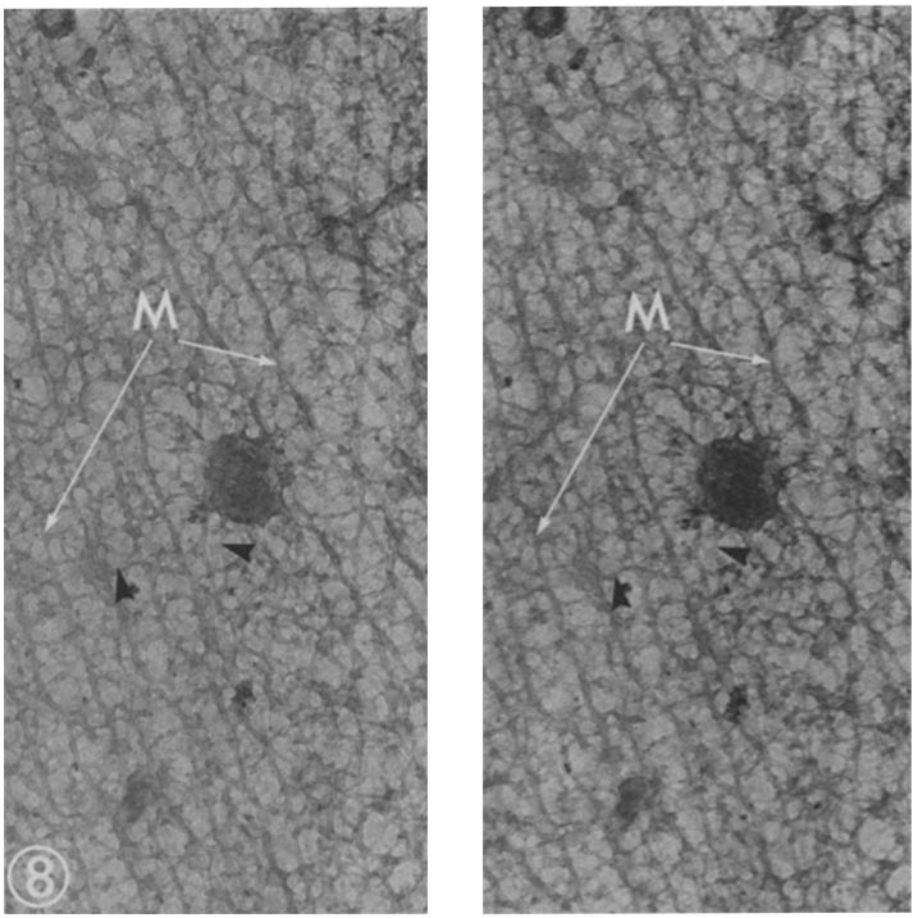

FIGURE 8 High-magnification stereo view of an axonal region in Fig. 6. The microtrabeculae (arrowheads) associated with the microtubules (*M*) are thicker and shorter and, as a result, the intermicrotubule distances are reduced. Here, a particle appears to be immobilized by numerous cross-linking trabeculae attached to its surface. × 49,000.

Possible Mechanism of Saltatory Transport

The observations made in this paper from stereo HVEM studies of hundreds of cells have been assimilated in a model in Fig. 10 describing possible mechanisms of particle transport in neurons. We propose that saltatory transport probably relies on cycles of localized, Ca^{2+}-triggered contractions and Mg^{2+}-dependent, ATP-requiring expansions of the microtrabecular lattice within Mt- and Nf-defined pathways. The onset of particle motion would occur with Ca^{2+}-stimulated detachments of trabeculae from the surfaces of organelles, thus releasing the particles so that they are pulled or pushed in the direction of least resistance, this being the direction of Ca^{2+}-stimulated contractions. Transport is discontinued when a moving particle(s) contacts an organized, expanded region of the lattice, where Mg^{2+}-induced attachments of the trabeculae serve to temporarily prevent further particle motion. We suspect that the SER and mitochondria operate to release and resequester small amounts of Ca^{2+} within Mt- and Nf-defined regions of the axoplasm to produce cyclic changes in organization of the lattice. The bidirectional nature of particle motion would reflect an ability of the lattice components to contract and expand in more than one direction along the linear Mts arrays. As the polarity of microtubules in neurons is predominantly unidirectional (24), this property could conceivably exert a polar effect on the overall direction of movement of axoplasmic organelles, since the majority of axonal transport in neurons is mostly away from the perikaryon.

The importance of intermicrotubule bridges or links in motility has been previously recognized in ciliary axonemes (19), and there is recent data showing that filaments will respond to Ca^{2+} and Mg^{2+} ions in vitro to bridge axonemal Mts (58). Similar types of links are seen in thin-section images of axoplasmic Mts, although the links tend to span greater distances to interconnect Mts with other Mts, with Nfs, and with organelles (6, 40, 57). On the basis of these types of studies, Metusals and Izzard (40) and Yamada et al. (57) originally envisaged these filaments to comprise a continuous three-dimensional network important for axoplasmic transport. A similar lattice was subsequently described by Burton and Fernandez (6) in crayfish axoplasm, and they suggested that Ca^{2+}-dependent contractile properties of a meshwork containing mucopolysaccharides may operate to provide the motive force for transport in neurons.

We believe that the filaments seen associated with Mts and Nfs in conventional thin sections make up at least a part of the complex lattice network associated with these structures in the HVEM results reported here. The lattice associated with Mts and Nfs probably constitutes a commonly shared axoplasmic component that is operative in axonal transport in diverse types of neurons. Porter and colleagues (8, 39) have discovered, in HVEM studies of pigmented cells derived from the neural crest, that pigment granules, like axoplasmic organelles, are contained in a continuous network of microtrabeculae associated with radial arrays of Mts. In these cells, pigment granule aggregation appears to depend on a synergistic contraction of the lattice components. Subsequent redispersions of granules in turn relies on a ATP-dependent reformation of microtrabecular networks (39). They suggested that properties of radially arrayed microtrabecular-Mt structures must provide the basic driving force for pigment granule motion.

In this study, attempts to determine whether changes in the organization of the axoplasm might precede and follow the passage of particles through a given region of the axoplasm

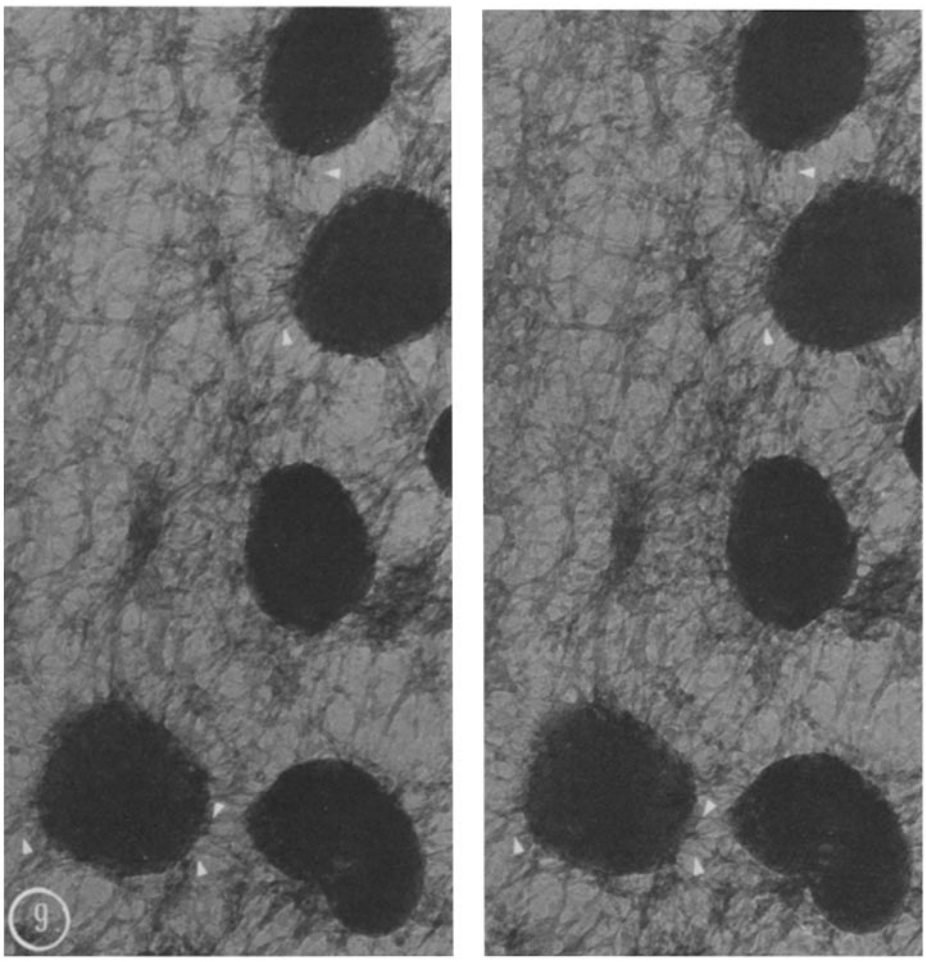

FIGURE 9 Shows part of an axon of a neuron exposed to 1 mM Mg^{2+} for 10 min. Transport was completely stopped at the time of fixation, apparently in response to a Mg^{2+}-induced elongation of trabeculae and the resulting gelated state of the microtrabecular lattice. Numerous thin filaments (arrowheads) are seen attached to the surfaces of organelles. Note that an abundance of assembled microtrabeculae makes it difficult to visualize microtubules. × 79,500.

TABLE III

Reactivation of Organelle Motion by Divalent Cations

Inactivating agent	Reactivating buffer	Recovery time
	mM	*min*
1 mM EGTA	HBSS	+10
	0.05 Ca ± 0.10 Mg	+5
	0.20 Ca ± 0.10 Mg	+2 / −5
	0.05 Ca ± 0.2 Mg	+2
	0.05 Ca + 2.0 Mg	+2 / −10
1 mM EDTA	HBSS	+10
	0.10 Mg ± 0.05 Ca	+5
	0.20 Mg ± 0.05 Ca	+2
	2.00 Mg ± 0.05 Ca	−1
	0.10 Mg + 0.20 Ca	+2 / −5

Summarizes the effects of exogenous Ca^{2+} and Mg^{2+} (mM levels) on the recovery of intracellular transport in neurons where transport was previously stopped using EGTA and EDTA at 1 mM in mHBSS containing 1 μg/ml A23187 for 20 min. Recovery with time is denoted by (+), and (−) means that transport was stopped at the time indicated.

have not yielded consistent results. In studies of the very thin regions of growth cones (<0.5 μm thick), for example, we have occasionally detected a coarsened (contracted) lattice in the direction of particle motion. Difficulties arise in assessing such differences, since the rate of transport is very rapid (1 μm/s) and small changes (contractions) of the lattice are probably sufficient to generate the movement of a particle. In this regard, the relatively slow rate of glutaraldehyde fixation may not permit adequate preservation of subtle organizational changes that occur in the lattice during transport. Thus, in order to learn more about lattice-regulated transport mechanisms, we experimentally manipulated physiological conditions thought to control the structural and functional properties of the lattice.

Divalent Cation Experiments

It is generally acknowledged that the mobilization of Ca^{2+} ions serves to regulate the activation of motility events ranging from muscle contraction, ameboid motion, and axonemal bending, to axonal transport. In neurons, Ca^{2+} (32) and ATP (43) depletion experiments have indicated that axonal transport is a Ca^{2+}-requiring, energy-dependent process. In this connection, Ca^{2+} was found to be essential for the onset of rapid transport (22) and shown to move bidirectionally with transported proteins (23). Further, Ca^{2+} concentrations have been localized in axoplasmic SER cisternae (25), and Ca^{2+}-binding proteins have been isolated from axoplasm (29). The studies have suggested that Ca^{2+}-loaded compartments could then serve to release and sequester Ca^{2+} ions to locally control intracellular motility in Mt channels. Ellisman and Porter (11) propose that vesicle release of Ca^{2+} from one end and sequestering at the other end could regulate the breakage and formation of trabeculae cross-linkages mediating their transport.

In this paper, time-lapse results from experimental manipulations of axoplasmic Ca^{2+} and Mg^{2+} ratios (using ionophore

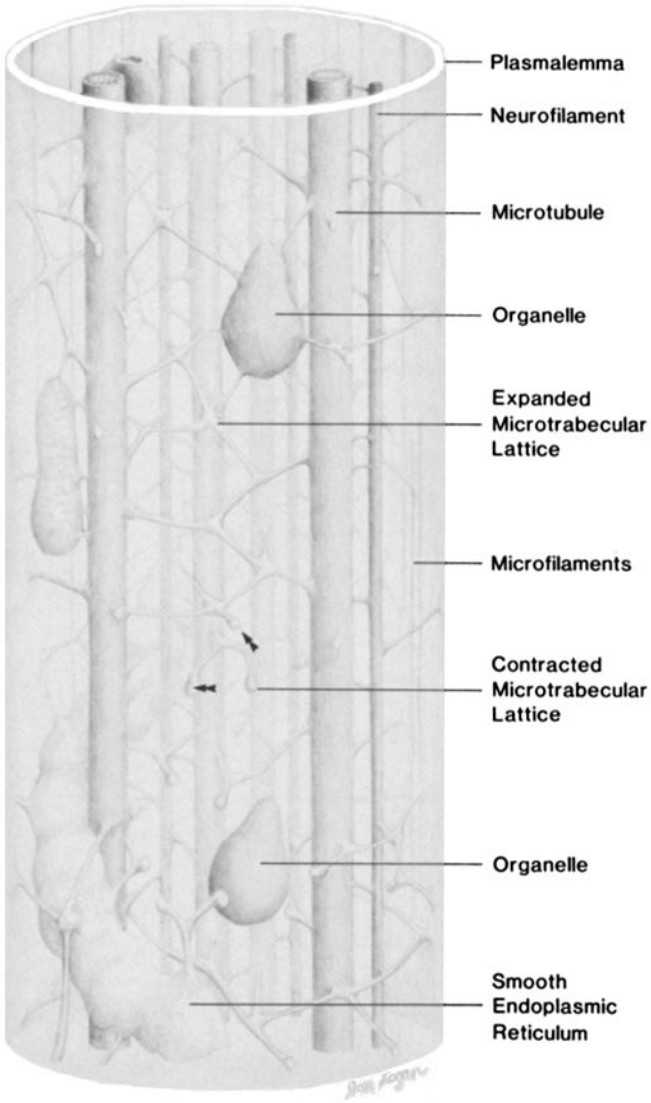

FIGURE 10 A model describing the structural organization of microtubules, neurofilaments, the cross-linking microtrabecular lattice, and other organelles in the axoplasmic matrix. The lattice emerges from the inner plasmalemmal surface to interconnect the surfaces of microtubules, neurofilaments, microfilaments, and other organelles. In response to a localized release of axoplasmic Ca^{2+} by the smooth endoplasmic reticulum, the thin, cross-linking trabeculae are believed to contract (double arrowheads) to somehow facilitate the saltatory movement of particle(s) in the direction of least resistance. We believe that the Ca^{2+}-contracted trabeculae may continue to interact with the particles but they do so without forming permanent attachments that would hinder movement. The duration of a saltatory event is limited by the extent of lattice contraction along defined microtubules. When an organelle encounters an expanded region of the lattice, Mg^{2+}-stimulated elongations and attachments of the trabeculae may momentarily prevent further motion. A Mg^{2+}-triggered, ATP-dependent reexpansion of trabeculae is proposed to immediately follow a given lattice contraction event. This would take place in preparation for the next contraction cycle upon the resequestering of Ca^{2+} ions by SER.

or chelating agents) have indicated that physiological shifts in Ca^{2+} and/or Mg^{2+} levels could indeed strongly influence axoplasmic transport events. The substitution of other ions such as Mn^{2+} or La^{+3} for Ca^{+2} and Mg^{+2} did not have a noticeable effect on the ultrastructure or behavior of neurons. Studies in other cell systems have demonstrated that the contraction of cytoplasmic matrices is sensitive to small increases in the free calcium ion levels (36, 41, 45). In pigment cells, for example, a slight elevation of the cytoplasmic concentration of Ca^{2+} was found to induce pigment aggregation, whereas reduced Ca^{2+} levels facilitated granule dispersion (38). In support of this idea, measurements made in this paper show that Ca^{2+} indeed can induce formation of trabeculae with thicker diameters (17.1 nm) and shorter lengths (93 nm), presumably representing a contracted state for the lattice.

The importance of Mg^{2+} ions in regulating cell motility is not understood as thoroughly as is the role of Ca^{2+}. In most studies, Mg^{2+} ions have been found to have a stabilizing effect on Mt systems in vivo (20, 45, 49). Shigenaka et al. (49), for example, have shown that microchondrial and granule motion in the axopodia of Heliozoans is discontinued in the presence of stabilizing levels of Mg^{2+} (0.07–10 mM). The data presented in this paper have revealed that, after brief Mg^{2+} starvation of cells, Mg^{2+} can produce similar effects in neurons by causing the assembly, elongation, and, ultimately, gelation of Mts and Mt-associated lattice components. Porter and Anderson (47) have recently reported that Mg^{2+} ions (1-mM levels) induce the formation of a finely divided lattice in cultured cells similar to the Mg^{2+}-lattice observed in neurons. We interpret the results to mean that Mg^{2+} is normally employed by the cell as a counterion to Ca^{2+} in order to maintain the lattice at its highest energy level. It is in this expanded state that the lattice has an ability to respond to Ca^{2+} ion fluxes that trigger the onset of organelle transport. Data presented in Table II support this proposal, showing that preincubation of cells with Ca^{2+} or Mg^{2+} ions can retard the effects of other ions.

Conclusions

The mechanism proposed here is in close agreement with several earlier models of axoplasmic transport (30, 44, 48, 49) where the movement of vesicles was proposed to occur by ATPase-dependent activities of cross-bridging MT-associated filaments. We believe that this basic concept of lattice-controlled transport is probably correct since it adequately accounts for several important features of axoplasmic transport which include: the specific association of particles with Mt or Nf bundles; the bidirectional, linear nature of saltatory events; and the sensitivity of transport and lattice organization to changes in Ca^{2+} and Mg^{2+} ion ratios.

Mt-directed saltatory motion may be augmented by localized contractions of subplasmalemmal networks in neurons. The Ca^{2+}-sensitive proteins, actin and myosin, have been identified in neurons by use of both fluorescently tagged antibodies (34) and a variety of EM techniques (1, 9, 36) including heavy meromyosin labeling (9). Isenberg et al. (30) and Goldberg et al. (22) have recently shown an inhibition of transport after the microinjection of the antimicrofilament agent DNase I into axons. Indeed, the HVEM images presented here have indicated that Mf bundles comprise part of the subplasmalemmal cytoskeletal network. Furthermore, recent in vitro viscometric studies have indicated that microfilaments can interact with microtubules coated with MAPs (microtubule-associated proteins) (21). It is reasonable to suppose then that Ca^{2+}-dependent interactions of microtubules, MAPs, and actin-myosin proteins could mediate transport in axons. Models that incorporate such lattice components would account for the observations that antimicrotubule and antimicrofilament drugs can both prevent and interfere with transport in neurons (see Fig. 10).

I thank Dave Boggs for excellent technical assistance. I am grateful to Dr. Richard McIntosh for critical reading of the manuscript.

The work was supported by a Canadian Muscular Dystrophy Association (MDA) postdoctoral fellowship to M. E. Stearn and MDA grant 1533765 to Dr. Keith Porter.

Received for publication 6 July 1981, and in revised form 6 November 1981.

REFERENCES

1. Berlinrood, M., S. M. McGee-Russell, and R. D. Allen. 1972. Patterns of particle movement in nerve fibers an analysis by photokymography and microscopy. *J. Cell Sci.* 11:875–886.
2. Borg, J., J. Mark, and P. Mandel. 1979. Effects of amino acids on calcium uptake by glial and neuroblastoma cells. *J. Neurobiol.* 10:31–40.
3. Brady, S. T., S. D. Crothers, C. Nosal, and W. O. McClure. 1980. Fast axonal transport of high Ca^{2+}: evidence that microtubules are not required. *Proc. Natl. Acad. Sci. U. S. A.* 77: 5909–5913.
4. Buckley, I. K. 1975. Three dimensional fine structure of cultured cells: possible implications of subcellular motility. *Tissue Cell* 7:51–72.
5. Buckley, I. K., and K. R. Porter. 1975. Electron microscopy of critical point dried whole cultured cells. *J. Microsc. (Oxf.).* 104:107–120.
6. Burton, P. R., and H. L. Fernandez. 1973. Delineation by lanthanum staining of filamentous elements associated with the surfaces of axonal microtubules. *J. Cell Sci.* 12:567–583.
7. Byers, M. R. 1974. Structural correlates of rapid axonal transport: evidence that microtubules may not be directly involved. *Brain Res.* 75:97–113.
8. Byers, R. H., and K. R. Porter. 1977. Transformations in the structure of the cytoplasmic ground substance in erythrophores during pigment aggregation and dispersion. I. A study using whole-cell preparations in stereo high voltage electron microscopy. *J. Cell Biol.* 75: 541–558.
9. Chang, C., and R. D. Goldman. 1973. The localization of actin-like fibers in cultured neuroblastoma cells as revealed by heavy meromyosin binding. *J. Cell Biol.* 57:867–874.
10. Douglas, W. W., and M. Sorimachi. 1972. Colchicine inhibits adrenal medullary secretion evoked by acetylcholine without affecting that evoked by potassium. *Br. J. Pharmacol.* 45: 129–132.
11. Ellisman, M. H., and K. R. Porter. 1980. Microtrabecular structure of the axoplasmic matrix: visualization of cross-linking structures and their distribution. *J. Cell Biol.* 87:464–479.
12. Fernandez, H. L., and F. E. Samson. 1973. Axoplasmic transport: differential inhibition by cytochalasin B. *J. Neurobiol.* 4:201–206.
13. Forman, D. S., A. L. Padjen, and G. R. Siggins. 1977. Axonal transport of organelles visualized by light microscopy: cinemicrographic and computer analysis. *Brain Res.* 136: 197–213.
14. Forman, D. S., A. L. Padjen, and G. R. Siggens. 1977. Effect of temperature on the retrograde transport of microscopically visible intraaxonal organelles. *Brain Res.* 136:215–226.
15. Freed, J. J., and M. M. Leobwitz. 1970. The association of a class of saltatory movements with microtubules in cultured cells. *J. Cell Biol.* 45:334–354.
16. Furcht, L. T., and R. E. Scott. 1975. Effect of vinblastine sulfate, colchicine and lumicolchicine on membrane organization of normal and transformed cells. *Exp. Cell Res.* 96: 271–282.
17. Gabbay, K. H., and W. J. Tze. 1972. Inhibition of glucose-induced release of insulin by aldose reductase inhibitors. *Proc. Natl. Acad. Sci. U. S. A.* 69:1435–1439.
18. Gauthier, L. M., D. Aronson, N. Gonsalves, and J. J. Diwan. 1980. Effects of DCCD, mersalyl, an oligomycin on mitochondrial K^+ and Mg^{2+} flux. *Fed. Proc.* 39:1705a.
19. Gibbons, B. H., and I. R. Gibbons. 1973. The effect of partial extraction of dynein arms on the movement of reactivated sea urchin sperm. *J. Cell Sci.* 13:337–357.
20. Goldberg, D. J., D. A. Harris, B. W. Lubit, and J. H. Schwartz. 1980. Analysis of the mechanism of fast axonal transport by intracellular injection of potentially inhibitory macromolecules: evidence for a possible role of actin filaments. *Proc. Natl. Acad. Sci. U. S. A.* 77:7448–7452.
21. Griffiths, L. M., and T. D. Pollard. 1978. Evidence for actin filament-microtubule interaction mediated by microtubule-associated proteins. *J. Cell Biol.* 78:958–965.
22. Hammerschlag, R., A. R. Dravid, and A. Y. Chiu. 1975. Inhibition of fast axonal transport of [^{3}H]-proteins by cobalt ions. *Neurosci. Abstr.* 1:801.
23. Hammerschlag, R., A. R. Dravid, and A. Y. Chiu. 1975. Mechanism of axonal transport: a proposed role of calcium ions. *Science (Wash. D. C.).* 188:273–275.
24. Heidemann, S. R. 1980. Visualization of the intrinsic polarity of microtubules. *J. Cell Biol.* 87 (2, Pt. 2): 245*a* (Abstr.).
25. Henkart, M., T. S. Reese, and F. J. Brinley. 1978. Endoplasmic reticulum sequesters Ca^{2+} in squid giant axon. *Science (Wash. D. C.).* 202:1300–1303.
26. Heslop, J. P. 1975. Axonal flow and fast transport in nerves. *Adv. Comp. Physiol. Biochem.* 6:75–163.
27. Hinkley, R. E. 1973. Axonal microtubules and associated filaments stained by alcian blue. *J. Cell Sci.* 13:753–761.
28. Hoffman, P. N., and R. J. Lasek. 1975. The slow component of axonal transport: identification of major structural polypeptides of the axon and their generality among mammalian neurons. *J. Cell Biol.* 66:351–366.
29. Iqbal, Z., and S. Ochs. 1975. Fast axoplasmic transport of calcium binding components in mammalian nerve. *Neuroscience* 1:802a.
30. Isenberg, E., P. Schubert, and G. W. Kreutzberg. 1980. Experimental approach to test the role of actin in axonal transport. *Brain Res.* 194:588–593.
31. Kirkpatrick, J. B. 1971. Time-lapse cinematography of axoplasmic flow in peripheral nerves. *In* Abstracts of the 11th Annual Meeting of the American Society for Cell Biology, New Orleans. 671a.
32. Kirkpatrick, J. B., and R. E. Rose. 1972. Calcium requirements for axoplasmic flow. *Proc. Am. Soc. Neurosci.* 1972:225.
33. Kreutzberg, G. W. 1969. Neuronal dynamics and axonal flow. IV. Blockage of intraaxonal enzyme transport by colchicine. *Proc. Natl. Acad. Sci. U. S. A.* 62:722–728.
34. Kuczmarski, E. R., and J. L. Rosenbaum. 1979. Studies on the organization and localization of actin and myosin in neurons. *J. Cell Biol.* 80:356–371.
35. Lane, N. J., and J. E. Treherne. 1970. Lanthanum staining of neurotubules in axons from cockroach ganglia. *J. Cell Sci.* 7:217–231.
36. LeBreton, G. C., R. J. Dinerstein, L. J. Roth, and H. Feinberg. 1976. Direct evidence for intracellular divalent cation redistribution associated with platelet shape change. *Biochem. Biophys. Res. Commun.* 71:362–370.
37. Lubinska, L. 1975. On axoplasmic flow. *Int. Rev. Neurobiol.* 17:241–296.
38. Luby, K. J. 1980. Both extracellular and intracellular Ca^{2+} play a role in the control of pigment migration in erythrophores of *Holocentrus. Eur. J. Cell Biol.* 22:352a.
39. Luby, K. J., and K. R. Porter. 1980. The control of pigment migration in isolated erythrophores of *Holocentrus ascensionis* (Osbeck). I. Energy requirements. *Cell* 21:13–23.
40. Metusals, J., and C. S. Izzard. 1969. Spatial patterns of threadlike elements in the axoplasm of the giant nerve fiber of the squid (*Loligo pealii* L.) as described by differential intereference microscopy and electron microscopy. *J. Cell Biol.* 43:456–479.
41. Moran, D., and R. W. Rice. 1976. Action of papaverine and ionophore A23187 on neurulation. *Nature (Lond.).* 261:497–499.
42. Ochs, S. 1972. Fast transport of materials in mammalian nerve fibers. *Science (Wash. D. C.).* 176:525–560.
43. Ochs, S., and D. Holingsworth. 1971. Dependence of fast axoplasmic transport in nerve on oxidative metabolism. *J. Neurochem.* 18:107–114.
44. Pomerat, C. M., W. J. Hendelman, C. W. Rainborn, Jr., and J. F. Masey. 1967. Dynamic activities of nervous tissue *in vitro. In* The Neuron. H. Hyden, editor. Elsevier, Amsterdam. 119–178.
45. Porter, K. R., and K. Anderson. 1980. Structural responses of the microtrabecular lattice (MTL) to changes in temperature, concentration of divalent cations and to cytochalasin. *Eur. J. Cell Biol.* 22:351a.
46. Samson, F. 1971. Mechanisms of axoplasmic transport. *J. Neurobiol.* 2:347–360.
47. Schmitt, F. O. 1968. Fibrous proteins—neuronal organelles. *Proc. Natl. Acad. Sci. U. S. A.* 60:1092.
48. Seeds, N. W., A. G. Gilman, T. Amano, and M. W. Nirenberg. 1970. Regulation of axon formation by clonal lines of a neural tumor. *Proc. Natl. Acad. Sci. U. S. A.* 66:160–167.
49. Shigenaka, Y., K. Watanabe, and M. Kaneda. 1974. Degrading and stabilizing effects of Mg^{2+} ions on microtubule containing axopodia. *Exp. Cell Res.* 85:391–398.
50. Smith, D. S. 1971. On the significance of crossbridges between microtubules and synaptic vesicles. *Philos. Trans. R. Soc. Lond. B Biol. Sci.* 261:295–405.
51. Tani, E., and T. Ametani. 1970. Substructure of microtubules in brain nerve cells as revealed by ruthenium red. *J. Cell Biol.* 46:159–165.
52. Trifaro, J. M., B. Collier, A. Lastoweka, and D. Stern. 1972. Inhibition by colchicine and by vinblastine of acetylcholine-induced catecholamine release from the adrenal gland: an anticholinergic action not an effect upon microtubules. *Mol. Pharmacol.* 8:264–267.
53. Wilson, L., J. Bryan, A. Ruby, and D. Mazia. 1970. Precipitation of proteins by vinblastine and calcium ions. *Proc. Natl. Acad. Sci. U. S. A.* 66:807–814.
54. Wolosewick, J. J., and K. R. Porter. 1979. Microtrabecular lattice of the cytoplasmic ground substance; artifact or reality. *J. Cell Biol* 82:114–139.
55. Wuerker, R. B., and J. B. Kirkpatrick. 1972. Neuronal microtubules, neurofilaments and microfilaments. *Int. Rev. Cytol.* 33:45.
56. Wunderlich, F., R. Muller, and V. Speth. 1973. Direct eivdence for a colchicine-induced impairment in the mobility of membrane components. *Science (Wash. D. C.).* 182:1136–1138.
57. Yamada, K. M., B. S. Spooner, and N. K. Wessells. 1971. Ultrastructure and function of growth cones and axons of cultured nerve cells. *J. Cell Biol.* 49:614–635.
58. Zanetti, N. C., D. R. Mitchell, and F. D. Warner. 1979. Effects of divalent cations on dynein cross bridging and ciliary microtubule sliding. *J. Cell Biol.* 80:573–588.